Materials Science & Engineering C 103 (2019) 109793

Contents lists available at ScienceDirect

Materials Science & Engineering C

journal homepage: www.elsevier.com/locate/msec

Membrane bioreactor for investigation of neurodegeneration

Sabrina Morelli[a,*], Antonella Piscioneri[a], Efrem Curcio[b], Simona Salerno[a], Chien-Chung Chen[c], Loredana De Bartolo[a,*]

[a] Institute on Membrane Technology, National Research Council of Italy, ITM-CNR, c/o University of Calabria, via P. Bucci cubo 17/C, I-87036 Rende, CS, Italy
[b] Department of Environmental and Chemical Engineering (DIATIC), University of Calabria, via P. Bucci cubo 45/A, I-87036 Rende, CS, Italy
[c] Institute of Biomedical Materials and Tissue Engineering, Taipei Medical University, Taipei, Taiwan

ARTICLE INFO

Keywords:
Poly-L-lactic acid membranes
Membrane bioreactor
Neuronal cells
Neuronal tissue engineered model
Glycitein
Alzheimer's disease

ABSTRACT

To gain a better understanding of neurodegeneration mechanisms and for preclinical evaluation of new therapeutics more accurate models of neuronal tissue are required.

Our strategy was based on the implementation of advanced engineered system, like membrane bioreactor, in which neurons were cultured in the extracapillary space of poly(l-lactic acid) (PLLA) microtube array (MTA) membranes within a dynamic device designed to recapitulate specific microenvironment of living neuronal tissue.

The high membrane permeability and the optimized fluid dynamic conditions created by PLLA-MTA membrane bioreactor provide a 3D low-shear stress environment fully controlled at molecular level with enhanced diffusion of nutrients and waste removal that successfully develops neuronal-like tissue.

This neuronal membrane bioreactor was employed as in vitro model of β-amyloid -induced toxicity associated to Alzheimer's disease, to test for the first time the potential neuroprotective effect of the isoflavone glycitein. Glycitein protected neurons from the events induced by β-amyloid aggregation, such as the production of ROS, the activation of apoptotic markers and ensuring the viability and maintenance of cellular metabolic activity.

PLLA-MTA membrane bioreactor has great potential as investigational tool in preclinical research, contributing to expand the available in vitro devices for drug screening.

1. Introduction

The control of neuronal in vitro networking is a challenging aspect in tissue engineering and its achievement comprises a variety of approaches that include static and dynamic in vitro devices. The engineered bioprocess of neuronal differentiation and alignment allows studying definite neuronal physiological or pathological events in a three-dimensional surrounding that can be, therefore, used as investigational tool for the evaluation of potential therapeutic strategy [1,2]. In this contest, nowadays, special demands come from the huge need of new treatments for neurodegenerative disease and with it the realization of biodevices to investigate new active molecules whose action can limit neurodegeneration exerting a neuroprotective effect [3].

The building up of an in vitro disease model system requires the development of a cellular microenvironment quite similar to the one of the native tissue involved in the investigated pathological situation. A promising and reliable model system indeed, has to allow the creation of an organized structure in which the proper cellular interaction and the native structural complexity are well established determining the acquisition and maintenance of the tissue functionality. The in vitro development of a neuronal tissue analogue requires a selective choice of the material that acts as a support in driving the formation of tissue-like structures [4,5]. The use of porous polymeric membranes comprises several advantages for the realization of these screening tools [6–10]. Highly porous polymeric membranes can be prepared in a tunable and controlled manner with reproducible characteristics in terms of physico-chemical and transport properties. Noteworthy, high level of porosity is particularly encouraged for 3D cell culture model; indeed a consistent porosity together with the pore interconnectivity ensure a uniform transport of the culture media within the whole cellular construct. Moreover, the intrinsic mechanical stability of the membrane confers also the proper strength for a long-term performance of the guiding biomaterial within the in vitro system. Membrane surface topography deeply influences the growth and migration of neuritis, therefore represents fundamental feature that enhances the physiological relevance of membrane application in neuronal tissue engineering. In addition, the membrane within a device ensures the

* Corresponding authors.
E-mail addresses: s.morelli@itm.cnr.it, sabrina.morelli@cnr.it (S. Morelli), l.debartolo@itm.cnr.it, loredana.debartolo@cnr.it (L. De Bartolo).

https://doi.org/10.1016/j.msec.2019.109793
Received 25 February 2019; Received in revised form 10 May 2019; Accepted 24 May 2019
Available online 26 May 2019
0928-4931/

appropriate transport of vital elements, such as nutrients, growth factors and oxygen, and is an ideal biomimetic interface able to promote neuronal adhesion and alignment according to a precise disposition. The presence of a microscale pattern at cell-membrane interface level not only promotes neuronal alignment according to a predefined path, but especially improves the overall neuronal performance in terms of morphological organization and specific metabolic functions leading to a better neuronal maturation and survival [4].

A main encountered limitation when designing an in vitro platform is the reproduction of the dynamic aspects of the tissue, which can be successfully overcome by the use of a perfused bioreactor able to boost the creation of an efficient 3D cellular construct. Optimized performance in terms of neuronal networking and differentiation can be achieved by the use of membrane bioreactors whose parameter setting ensures an efficient neuronal growth and consequently a fully maturation in terms of processes extension and specific differentiated functions. One of the major issues faced when working with membrane bioreactor is membrane fouling, which could significantly reduce membrane performance and lifespan, resulting in a significant increase in maintenance and operating costs [11–13]. Despite the big impact of this issue on membrane operational systems, it didn't affect membrane bioreactor performance in the field of tissue regeneration, as corroborated by the achievement of morphological and functional neuronal differentiation [14,15]. Within a membrane bioreactor, by varying configuration and membrane properties, several critical issues can be controlled and adjusted according to a precise setting, thus offering to the cells a proper supply of gases, nutrients and the removal of waste products [16]. Furthermore, hollow fiber-based bioreactors are preferable to other designs for the culture of neurons due to the large surface area for cell adhesion to volume ratio and the indirect perfusion of cells protecting them from shear stress [14,17], compared to other devices that are based on a direct perfusion [18,19].

In this paper, we report the successful integration of a membrane bioreactor technology and an efficient neuronal differentiation for the realization of a highly performing in vitro membrane investigational platform to model neurological disorders as Alzheimer's disease together with the screening of new molecules that can stop or delay the progression of the associated neurodegeneration. Our strategy aims to generate a new 3D neural disease model contributing to expand the available in vitro tools for drug screening.

Considerable achievements have been reached in optimizing electrospun membrane and their tunable characteristics. Intrinsic electrospun membrane properties mimic the nano and microscale features of the extracellular matrix resulting in a suitable biomaterial for cell support promoting a proper cellular organization [20]. The use of these membranes in tissue engineering and regenerative medicine must be adopted to the natural organization of the cells or to the specific final application and in the case of neuronal tissue engineering the use of aligned fibers is strongly encouraged and particularly appealing to enhance the topographical support in promoting a neuronal alignment. In this work, we used porous poly (l-lactic acid) (PLLA) microtube array (MTA) membranes prepared through a co-axial electrospinning process. They are distributed according to a single layer of hollow fiber membranes highly packed and aligned that showed also an optimal behavior in promoting neuronal adhesion and differentiation. Recently, excellent results were achieved by using MTA membrane bioreactor for the realization of a neuronal network whose spatial organization followed membrane's direction thus giving arise to an aligned disposition of the growing neuronal process [15]. Our previous study represents the proof of concept to validate the use of the PLLA-MTA membrane bioreactor as a reliable neuronal culture system for the in vitro disease modelling of Alzheimer to test for the first time the potential neuroprotective effect of a natural compound, the isoflavone glycitein. The main goal of the present work was to demonstrate that the PLLA-MTA membrane bioreactor, beside boosting an organized disposition of the neuronal network development and sustaining the all-biological functions, is also a suitable tool for the delivery of specific compounds and drugs at cellular compartment level whose action can be investigated in a neuronal tissue construct raised in a biologically realistic environment. To achieve this purpose, the enhanced transport properties of the membrane bioreactor were investigated by performing several permeability tests to different compounds including the glycitein that in tandem with the constant perfusion offered by the bioreactor give arise to a totally controlled and reliable biodevice. A modelling study was performed in order to outline the concentration profiles of specific neuronal metabolites as a function of an efficient mass transfer of nutrients across the microporous PLLA-MTA membranes within the bioreactor. The optimized setting parameter of the membrane device and the controlled environment at molecular level allowed the culture of neuronal cells by guiding cell orientation and differentiation as well as long term maintenance of metabolic activity in order to create an in vivo-like neuronal tissue. Importantly, neuronal PLLA-MTA membrane bioreactor was thus employed as a tool mimicking the toxicity associated to Alzheimer's disease caused by amyloid beta (Aβ) peptide aggregation, to perform a multifunctional analysis of the glycitein's anti-amyloidogenic effects on Alzheimer diseased neurons. The overall application represents therefore a promising resource to use membrane bioreactor technology as preliminary drug screening in vitro tool for the use of new therapies to treat neurodegenerative disorders facing at the same time, the challenging issues of reducing costs and animal experiments as well as shortening time for their introduction to the market.

2. Materials and methods

2.1. Materials

Poly(l-lactic acid) (PLLA) was purchased from BioTechOne (San Chung, Taiwan); human neuroblastoma cell line SH-SY5Y was obtained from ICLCIST (Genova, Italy); Accu-Chek Active assay was purchased from Roche Diagnostics (Monza, Italy); Brain derived neurotrophic factor (BDNF) ELISA immunoassay from Promega (WI, USA); Beta-amyloid $_{1–42}$ (Aβ)-Hexafluoroisopropanol (HFIP) fragment was purchased from Anaspec; Minimum essential Eagle's medium (EMEM) and fetal bovine serum were purchased from Lonza (Basel, Switzerland). Ham's F12 and secondary antibodies were purchased from Invitrogen (Milan, Italy). Neuron-specific mouse anti-β-III tubulin/TuJ1 and anti-synaptophysin antibodies were obtained from Chemicon (Millipore, Milan, Italy). Penicillin and streptomycin were purchased from Biochrom AG (Berlin, Germany); anti-growth associated protein 43 (GAP43) and anti-phospho-c-Jun N-terminal Kinase (JNK) antibodies were purchased from Santa Cruz Biotechnology (Santa Cruz, Calif., USA). Caspase-3 antibody was obtained from BD (Franklin Lakes, N.J., USA); polyethylene glycol/polyethylene oxide (PEG/PEO), 2′,7′-dichlorodihydrofluoroscein diacetate (H_2DCF-DA), 3-[4,5-dimethylthiazol-2-yl]-2,5-diphenyltetrazolium bromide (MTT), Hanks' solution, L –glutamine, glutamine, Glucose, retinoic acid, glycitein and other chemicals were obtained from Sigma Aldrich (Milan, Italy).

2.2. Membrane bioreactor

The bioreactor consists of a specially designed bioreactor chamber with two opposite transparent glass windows in which two layers of contiguous PLLA-MTA membranes are assembled in parallel to create an intraluminal and an extraluminal compartment, within the microtubes and in the shell, respectively, with a membrane surface area of 7,12 cm^2, for cell adhesion and growth, and a volume of 2.4 mL. There are 4 ports total: one for medium inlet leading to membranes, one for medium outlet leading from membrane bundle, and two ports located directly at the top and the bottom of the housing directly connected to the cell compartment and were used for cell seeding. The bioreactor is connected to the tubing circuits by using a micro-peristaltic pump to perfuse culture medium and oxygen through the membranes within the

Table 1
PLLA-MTA membrane bioreactor conditions: Volume bioreactor V_{BR}; Perfusion flow rate Q; Transmembrane pressure ΔP™; Reynolds number Re.

Membrane area [cm^2]	7.12
V_{BR} [mL]	2.4
Q [mL/min]	0.37
ΔP™ [mbar]	75
Mean retention time [min]	6.4
Re	0.18

chamber.

This configuration creates an in vitro environment that mimics the in vivo configuration of blood supply through capillary network beds in order to maintain dynamic homogeneous nutrition and gas exchange in order to allow tissue formation.

The flow rate was set to 0.37 mL/min on the basis of the average retention time and fluid dynamic characterization. Fresh medium was perfused in single-pass and the stream leaving the bioreactor was collected as waste until approaching the steady state (mean retention time, 6.4 min), when the concentration of the perfusion medium at all points in the bioreactor reaches a constant level, then the stream leaving the bioreactor was recycled in order to obtain the accumulation of products. Table 1 provides information regarding the membrane bioreactor operating parameters.

2.2.1. Preparation of PLLA-MTA membranes

PLLA-MTA membranes were prepared by electrospinning process, as previously reported [17]. Briefly, the shell solution of 10 wt% of PLLA/PEG (ratio: 7/3 wt%) was prepared by dissolving the respective components in a co-solvent of DCM/DMF (8:2 wt%) [21]. The resulting solution was co-axially electrospun with the core solution (10 wt% PEO/PEG in ddH_2O) at a flow rate of 4–10 mL h^{-1}, delivered by syringe pumps (KDS-100, KD Scientific, Holliston, MA, USA); a voltage of 4–8 kV, supplied by an electrostatic generator (You-Shang, Fongshan City, Taiwan) onto a collection drum with a rotation speed of 100 rpm under ambient conditions. The resulting membranes, were retrieved and soaked in ddH_2O for 24 h, followed by air-drying.

2.2.2. Characterization of PLLA-MTA membrane properties

The morphology of the electrospun hollow fibers was observed by a scanning electron microscope (SEM, ESEM FEG QUANTA 200, FEI Company, Oregon, USA). The diameters of the fibers and their porosity were measured on the SEM images using image analysis software (NIH-Scion Image).

The mean pore size and pore size distribution of the PLLA-MTA membranes, were determined by a Capillary Flow Porometer CFP 1500 AEXL (Porous Materials Inc. PMI, Ithaca, New York, USA).

The hydrophobic/hydrophilic membrane character was evaluated via dynamic contact angle measurements with CAM 200 contact angle metre (KSV Instruments, Ltd., Helsinki, Finland).

Mechanical properties of the electrospun aligned PLLA hollow fibers were determined using a Zwich/Roell Z2.5 tensile testing machine (Germany), as previously reported [22]. Young's modulus, tensile strength, and elongation at break parameter were obtained from the stress/strain curves.

The mass transport properties of PLLA-MTA membranes were characterized by performing permeance measurements of water, and different nutrients as neuronal culture medium, and solutions of some components of the culture medium, such as glucose and glycitein.

A peristaltic pump (ISMATEC, General Control, Milan, Italy) circulated the metabolite solution by pumping the fluid (feed) from the reservoir into the inlet port of the bioreactor. Pressures were monitored at inlet and outlet of the bioreactor by manometers (Allemano, accuracy ± 0.98 mbar). Inlet pressures were varied in order to obtain transmembrane pressures (*ΔP*™) from 0 to 175 mbar. The extraluminal flow, permeate, of the different test solutions was measured continuously. Neuronal culture medium was composed by a 1:1 mixture of Ham's F12 and EMEM enriched with a 5%(v/v) of heat inactivated foetal calf serum, 2 mM glutamine, 100 μg/mL penicillin–streptomycin. Test solutions of glucose and glycitein were prepared by dissolving separately 1.8 g/L of glucose and 100 μM of glycitein in phosphate buffer at pH 7.4. The PLLA-MTA membrane bioreactor was initially fed with water to evaluate the hydraulic permeance, and then it was filled with metabolite solutions for solute permeation measurements. For each type of metabolite a new system was used. In order to ensure a high reproducibility of permeance data, transmembrane flux versus *ΔP*™ was evaluated on three modules and the average permeance was reported.

Diffusive transport of glucose and glycitein from the fiber lumen to the shell side of PLLA-MTA membranes were also evaluated by assessing changes with time of their concentrations in the shell. The concentration of glycitein permeating through the membranes was monitored by an online UV-spectrophotometer (UV Cord Pharmacia, Uppsala, Sweden); glucose concentration was determined by using Accu-Chek Active assay.

2.3. Cell culture and neuronal differentiation assessment

The human neuroblastoma cell line SH-SY5Y was cultured at the density of 5×10^4 cell/cm^2 in the extracapillary space of the PLLA-MTA membranes within the bioreactor and maintained in a 5% CO_2/37 °C incubator (PBI international, Milan, Italy) up to 14 days. After 24 h the culture medium was changed and replaced with a fresh Ham's F12-EMEM containing 10 μM retinoic acid to promote the differentiation of SH-SY5Y towards neuronal phenotype, as previously reported [23]. Fresh medium was constantly provided to the cells.

Cell differentiation towards a neuronal phenotype was investigated by evaluating cell morphology and the expression of specific neuronal markers, by SEM analysis and immunostaining, respectively.

For morphological observation, the SEM preparation procedure involved fixing the samples of cells grown onto PLLA-MTA membranes within the bioreactor with a 3% solution of glutaraldehyde, treatment with 1% osmium tetroxide, and alcohol dehydration followed by drying. Samples were examined using SEM in order to investigate the effects of electrospun hollow fibers on cell morphology under dynamic conditions. Representative images displaying cell adhesion, growth, spreading and distinct neuronal structural features, such as neurite processes, synapses, axons and neuronal network formation, were obtained after 14 days of culture on the PLLA-MTA membrane surface within the bioreactor.

Immunostaining procedure was first carried out by fixing cells in 4% (wt/v) paraformaldehyde for 30 min, followed by permeabilization and blocking with a solution containing 0.3% (v/v) Triton X-100 and 10% (v/v) FBS in PBS for 1 h at 37 °C. Samples were then incubated overnight at 4 °C with the primary antibodies namely anti-Tuj1 (anti rabbit, 1:500), anti- synaptophysin (anti mouse, 1:400) and anti-GAP43 (anti goat, 1:200) which are specific for cytoskeleton protein βIII -tubulin, synaptophysin and axonal growth protein GAP 43, respectively. A Cy2™-conjugated Affini Pure donkey anti-rabbit IgG, a Cy3™-conjugated Affini Pure donkey anti-mouse IgG and a and Cy5™-conjugated Affini Pure donkey anti-goat IgG were then added at 1:500 dilution for 1 h at RT. Finally, cells were counterstained with 200 ng/mL DAPI for nuclear localization.

Confocal Laser Scanning Microscope (CLSM, Fluoview FV300, Olympus, Italy) was used to visualize the immunohistochemical staining of neuronal cells. Confocal laser images of neuronal cells after 14 culture days within the bioreactor, were analyzed to investigate the ability of the dynamic membrane device in allowing the differentiation of neuronal cells. In particular, the analysis of the distribution pattern profile of the neuronal specific markers, βIII-tubulin, GAP-43 and synaptophysin, was carried out in order to demonstrate that cells in the

bioreactor acquired specific neuronal morphological and functional features in terms of neuronal sprouting, axonal growth, synaptic and neuronal network formation.

2.4. Biochemical assays

The metabolic activity of neuronal cells was evaluated by investigating glucose consumption, and the neuronal brain-derived neurotrophic factor (BDNF) production in the medium collected during the culture time in the extracapillary space of the PLLA-MTA membranes within the bioreactor.

The glucose concentration and consumption were detected by using Accu-Chek Active glucose meter which measures glucose levels based on enzymatic reaction by means of appropriate test strips.

To assess BDNF secretion, a BDNF ELISA immunoassay was carried out according to the manufacturer's protocol. Briefly, ELISA plates were coated with anti-BDNF monoclonal antibody overnight at 4 °C. After washing, 100 µL of sample was added to the wells and left for 2 h at room temperature. Thereafter the wells were incubated with anti-human BDNF for 2 h at room temperature. After washing five times the wells were covered for 1 h with anti-BDNF antibody horseradish peroxidase conjugate and then tetramethylbenzidine was added. The reaction was blocked with 1 N HCl and absorbance was measured at 450 nm using a Multiskan Ex (Thermo Lab Systems).

2.5. Modelling

A mathematical modelling was implemented with the aim to describe the time-variant concentration profiles of glucose and BDNF as a result of mass transfer and reactions taking place in the MTA membrane bioreactor.

Concentration profiles were obtained by solving the unsteady-state diffusion/reaction problem described by the following set of partial differential equations (PDE) for incompressible Newtonian fluids:

i) continuity equation:

$$\nabla \cdot u = 0 \tag{1.a}$$

ii) momentum equation (absence of external force acting on the system):

$$\frac{\partial u}{\partial t} = -(u \cdot \nabla)\, u + \nu \nabla^2 u - \frac{1}{\rho}\nabla p \tag{1.b}$$

iii) mass transfer and reaction within the cellular compartment:

$$\frac{\partial c}{\partial t} + (u \cdot \nabla c) = D_{eff}\, \nabla^2 c \pm \Psi \tag{1.c}$$

where u is the velocity vector, t the time, ν is the kinematic viscosity, ρ is the fluid density, p the pressure, c is the molar concentration, D_{eff} is the effective diffusion coefficient in the cellular compartment, and Φ the reaction rate per unit volume (negative for glucose uptake and positive for BDNF production).

Eqs. (1.a)–(1.b) are formulated for incompressible Newtonian fluid, laminar flow regime and constant fluid density. Boundary conditions include:

i) the specification of the inlet velocity $u_0 = 0.2$ cm/s, evaluated as the ratio between the inlet flowrate (0.37 cm^3/min) and the total cross-section area of the microtube array membranes ($4.5 \cdot 10^{-5}$ cm^2), with ~ 130 microtubes/cm and single microtube average diameter of 76 µm);
ii) atmospheric pressure at the bioreactor outlet;
iii) transmembrane flow velocity according to Darcy's law.

Eq. (1.c) was numerically solved for the following boundary conditions:

i) $c(t = 0) = c_0$ at the inlet of the intraluminal compartment (c_0: initial concentration, i.e.1.3 mg/mL for glucose, 0 for BDNF), and c (t = 0) = 0 throughout the whole extrafiber space;
ii) $-D_{eff}\nabla c + u \cdot c = 0$ at the membrane interface;
iii) $\nabla c = 0$: insulation/symmetry condition for all remaining boundary surfaces.

PDE was numerically integrated by COMSOL MULTIPHYSICS Chemical Engineering Module, using Finite Elements Method (FEM) with Damped Newton algorithm for matrix factorization (tolerance for convergence of 10–6). In order to decrease the computational complexity of the system, two adjacent microtube membranes of the array were considered as simulation elements. Discretization by adaptive tetrahedral mesh generation procedure resulted into ~4244 nodes and solved for 8625 degrees of freedom.

The theoretical analysis was protracted until the thirteen day of culture, and results compared to the experimentally measured data.

2.6. Cell treatments: β-amyloid toxicity and Glycitein administration

To establish the toxic model of Alzheimer's disease, the differentiated neuronal cells at day 7 of culture in PLLA-MTA membrane bioreactor were exposed to the culture medium containing 5 µM of β-amyloid $_{1–42}$ (Aβ) peptide. To evaluate the effects of glycitein on Aβ-induced toxicity, cells were then treated with a mixture of Aβ (5 µM) and Glycitein at different concentrations (25, 50 and 100 µM) for 24 h at 37 °C.

Aβ-HFIP was dissolved in dimethylsulfoxide (DMSO) to have a stock solution of 1 mg/mL concentration, diluted to 25 mM in PBS, pH 7.4, and incubated for 24 h at 37 °C.

Glycitein was dissolved in DMSO to have a 1 mM stock solution and added to the culture medium at the indicated concentrations.

2.7. Assessment of cell viability

Cell viability was evaluated by using the colorimetric 3-(4,5-dimethylthiazol-2- yl)- 2,5-diphenyltetrazolium bromide (MTT) test. Cells were incubated with medium containing MTT solution (5 mg/mL) for 2 h at 37 °C, and the formazan particles were dissolved with lysis buffer (10% SDS, 0.6% acetic acid in DMSO, pH 4.7). The quantity of formazan product was directly proportional to the number of metabolically active living cells. The optical density was spectrophotometrically measured at 570 nm. Results obtained under the different treatments were expressed as the percentage of the control consisting of cells cultured in the membrane bioreactor without any treatment.

2.8. Measurement of intracellular reactive oxygen species (ROS) generation

Intracellular ROS were measured by using fluorescence assay with 2′,7′-dichlorodihydrofluoroscein diacetate (H_2DCF-DA). This molecule is hydrolyzed by intracellular esterases and then oxidized by interacting with ROS to give the highly green fluorescent DCF. Accumulation of DCF in cells can be measured by an increase in fluorescence which is proportional to the ROS level. In our experiments the oxidation of this probe was detected by monitoring the increase in fluorescence with a Confocal Laser Scanning Microscope (CLSM, Fluoview FV300, Olympus, Milan, Italy), using an argon laser. In particular, the neuronal cells in the membrane bioreactor after 24 h of treatment with Aβ and the different concentration of glycitein were incubated with H_2DCF-DA (50 µM) for 30 min at 37 °C, then cells were washed twice with Hank's salt solution, and finally the fluorescence's intensity of DCF was measured with CLSM. A quantitative analysis was performed on CLSM images of cells by using Fluoview 5.0 software (Olympus Corporation).

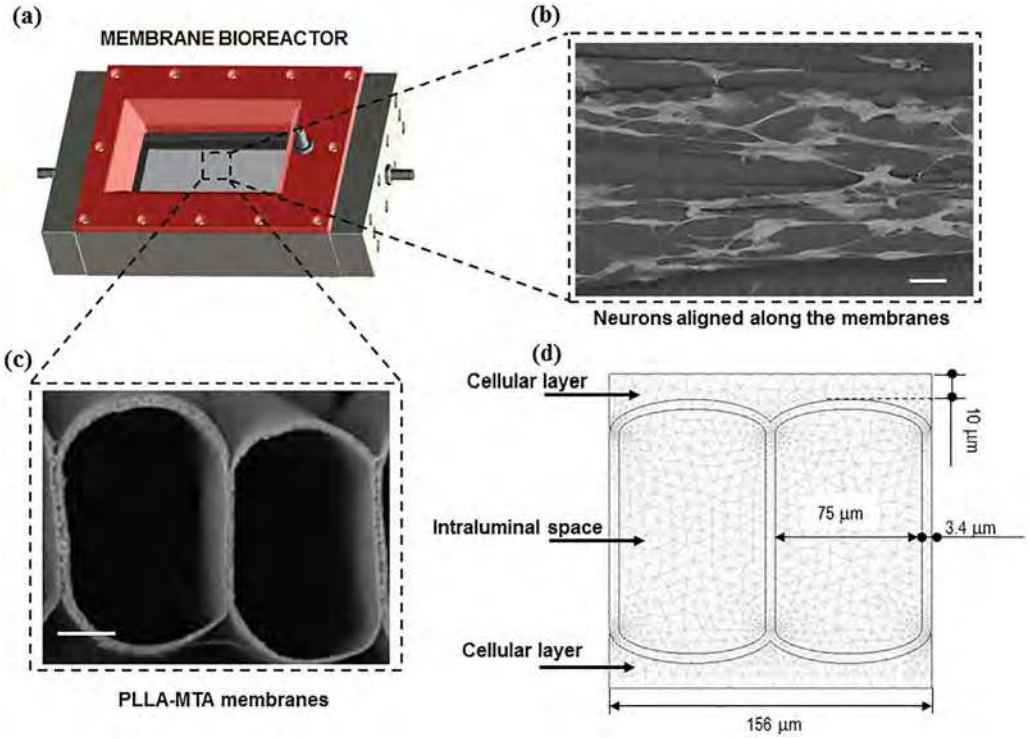

Fig. 1. PLLA-MTA membrane bioreactor (a), SEM micrographs of neuronal cells adhered onto the extrafiber surface of PLLA-MTA membrane within the bioreactor after 13 days of culture (b), andPLLA-MTA membranes (c), Computer-assisted design of the simulated element of the bioreactor (d). Scale bar = 30 µm.

2.9. Apoptosis assay

The expression and distribution of two apoptotic markers, caspase-3 and phospho-JNK (p-JNK), were examined by immunofluorescence technique using a rabbit anti-caspase-3 antibody (1:250) and a mouse anti-p-JNK (Thr183/Tyr 185) antibody (1:250), respectively, through CLSM investigation. A quantitative analysis was performed by direct counting the numbers of caspase-3 and JNK positive nuclei (apoptotic) and DAPI-stained (total) nuclei for the different treatments. For each apoptotic marker the percentage of apoptotic cells was calculated as the ratio of apoptotic cells (caspase-3 positive or p-JNK-positive cells) over total nuclei (DAPI-stained nuclei) counted at different culture conditions. Different areas were selected for the analysis of fifteen images for each culture condition of 3 independent experiments.

2.10. Statistical analysis

The statistical significance of the experimental results was calculated using an ANOVA test followed by a Bonferroni *t*-test ($p < 0.05$).

3. Results and discussion

3.1. PLLA-MTA membrane bioreactor properties

Current research in the field of neuronal tissue engineering aims to mimic the mature neuronal tissue microenvironment since there is a clear need for more accurate in vitro models of the human nervous system due the current lack of efficient treatments for neurological disorders.

A variety of advanced materials and devices have been investigated for generating neuronal tissue-like constructs, but to date, the research is very far from the introduction of 3D neural tissue products on the public market. Bioreactor-based strategies have been recognized as reliable systems and are attracting growing interest for creating investigational tools for the treatment of neurodegenerative diseases [14,24]. Membrane bioreactors compared to the other traditional bioreactor used for neuronal growth, as stirred tank, rotating wall and microperfused bioreactors [18,19,25,26], have the advantage to ensure uniform nutrient and metabolite exchange in the cell compartment protecting cells from shear stress thanks to the indirect perfusion [14,17].

In the present study, we developed a membrane bioreactor to serve as advanced investigational platform replacing traditional 2D cell culture systems or animal experiments for preliminary screening of the potential neuroprotective effect of a phytoestrogen, the isoflavone glycitein.

Based on a proof of concept [15], we successfully fabricated a neuronal tissue-like system by integrating PLLA-MTA membranes within a dynamic system to create a fully controlled in vitro microenvironment. The bioreactor consisted of a specially designed chamber in which PLLA-MTA membranes were assembled in parallel and connected to the perfusion system in order to create an intraluminal compartment for the medium flux, and an extraluminal one for the culture of neuronal cells. The two separate compartments communicate through the pores of the membranes that allow the delivery of metabolites towards the cells and the removal of secreted products. For the achievement of a complete membrane platform design, the membrane must possess defined characteristics since it plays a pivotal role for the overall performance of the bioreactor system.

Different parameters, including membrane structural characteristics, physico-chemical, mechanical and transport properties, as well as fluidynamics of the bioreactor were studied to investigate and optimize the conditions required for an efficient culture of neurons. PLLA-MTA membrane structure consists of electrospun hollow fibers, which are one by one packed and highly aligned to form a contiguous microtube array with an extremely high degree of fiber alignment. SEM analysis of the cross section displays a porous structure (Fig. 1c) characterized by a mean pore size diameter of 0.36 ± 0.14 µm, and a porosity of 46 ± 7%, with high pore interconnectivity. The membranes have an internal and external diameter of 75 ± 8 µm and 78 ± 10 µm,

respectively, and a very thin wall thickness of 3.4 ± 0.7 μm.

It is noteworthy that membrane physico-chemical and mechanical properties play important roles in regulating neuronal tissue formation [23,27], hence, we also evaluated these critical parameters of PLLA-MTA membranes. The water contact angle measurements demonstrated a moderate surface wettability with advancing and receding contact angle values of 87.3 ± 3° and 50.1 ± 2.5°, respectively. The membranes also exhibited an adequate mechanical properties in terms of Young modulus (Emod), Ultimate tensile strength (UTS), and Elongation at break parameter (ε) that are 78.8 ± 4.7 MPa, 1.8 ± 0.1 MPa and 10.3 ± 2.1%, respectively.

In tissue constructs cell behavior is influenced not only by cell-cell and cell-material interactions, but also by the proper supply and availability of sufficient quantity of nutrients in order to maintain viable and functioning neuronal cells. Membrane bioreactors must provide adequate mass transport of nutrients, metabolites and oxygen to the cells, and in the same time, it must allow rapid removal of metabolic products from the cellular environment. To assess the adequate inflow and outflow of the different elements, permeation of biological compounds through membranes needs to be carefully investigated to better enhance the overall cell growth and differentiation within the bioreactor. The evaluation of the mass transport rates of target molecules through the microporous PLLA-MTA membranes within the bioreactor was carried out. Solutions of different nutrients and metabolites were circulated by means of the tubing circuit, and perfused through the membranes within the bioreactor chamber from the intraluminal compartment, where the culture medium flows, to the extraluminal one, where the cells adhere. In order to investigate their effective transport towards the neuronal compartment, the transmembrane flux of culture medium, glucose, and glycitein solutions, which are crucial for neuronal outgrowth, were measured and compared with hydraulic permeance (Fig. 2a).

The steady-state hydraulic permeance of the membranes, calculated as the slope of the flux (J) versus transmembrane pressure (ΔP™) straight line, was 1.22 L/m^2 h mbar, with an R-squared value of 0.99. Permeation measurements of the different metabolite solutions through the membranes are reported in Fig. 2. The values of the permeances were 0.98 L/m^2 h mbar (R^2 = 0.98) for glucose solution, 0.94 L/m^2 h mbar (R^2 = 0.99) for culture medium, and 0.76 L/m^2 h mbar (R^2 = 0.99) for glycitein solution. The permeation rate of culture medium through PLLA-MTA membranes was close to the corresponding value of glucose solution and significantly higher than glycitein solution. This result could be related to the membrane physico-chemical properties since membrane transport properties are deeply influenced by interactions between permeating species and polymeric surfaces. Indeed, in our study, the proteins of the culture medium significantly modified the values of both contact angles and components of surface tension of the PLLA-MTA membranes [15]. After 24 h of incubation in culture medium containing serum proteins, the static contact angle of the membranes (θ_W: 88.2 ± 5.5°) significantly decreased (52.4 ± 6°), while the base parameter γ^- of surface tension, which is indicative of membrane hydrophilicity [28] increased, due to the protein adsorption. As a result, PLLA-MTA membranes acquire a more hydrophilic character in culture medium that probably lead to an increase in transmembrane flux with respect to the glycitein solution. The permeance of glucose and glycitein is also influenced by their chemical structure, molecular size and interaction with the membranes. The transmembrane flux decreased with increasing their molecular weight (MW), in accordance with previous works [29]. Indeed, the flux for glucose (MW 180 Da) solution was significantly greater than that of glycitein (MW 284 Da) solution.

To further investigate the transport properties of our dynamic device in order to demonstrate an efficient supply of target molecules to cell compartment, concentration profiles of glucose and glycitein permeating through PLLA-MTA membranes have been monitored in the extrafiber space within the bioreactor. For both molecules, the

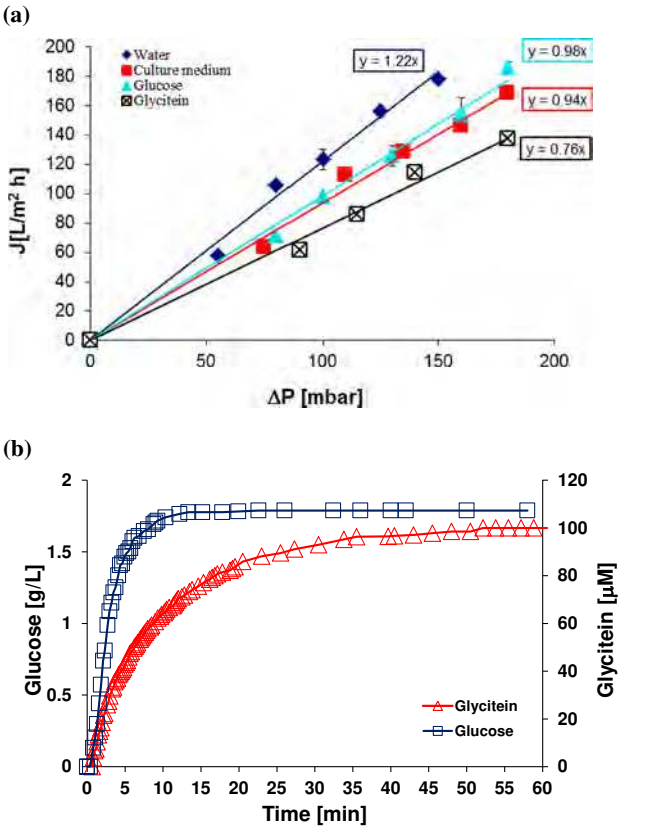

Fig. 2. Transport properties of PLLA-MTA membranes: Permeation measurements of water and metabolites through the membranes (a); Concentration appearance profiles of Glucose and Glycitein solutions in the extrafiber space of PLLA-MTA membranes within the bioreactor (b).

concentration increased with time and reached a plateau, as it is reported in the graph in Fig. 2b. In particular, metabolite solutions diffused from the lumen to the shell compartment through the fiber wall of PLLA-MTA membranes and the concentrations reached the plateau after 23 min for glucose, and after 52 min for glycitein solutions, respectively.

Since glucose is the main source of energy for brain tissue, the availability of glucose and its transport to the neuronal cells is critical for maintaining normal physiological brain functions. We provided several evidences that the PLLA-MTA bioreactor was able to allow the transport of such energetic fuel of brain. These findings clearly indicate that PLLA-MTA membrane bioreactor is suitable of providing adequate levels of nutrients supply and metabolites mass transfer that are essential for maintaining cell viability and ensure the growth and differentiation of neuronal cells.

3.2. PLLA-MTA membrane bioreactor provides an efficient environment for the long-term maintenance of differentiated neuronal cells

Building upon our previous work [15], an important aim of the present study is to provide further evidences confirming the capacity of the advanced membrane bioreactor to create a homogeneous and stable in-vivo-like neuronal microenvironment that could be employed as investigational platform. To pursue this goal, neuronal cells were cultured within PLLA-MTA membrane bioreactor and maintained for up to 2 weeks in order to assess the ability of the dynamic membrane device in allowing the long-term growth and differentiation of neuronal cells.

Cellular morphology was monitored and neuronal differentiation efficiency evaluated along the culture time. Scanning electron micrographs reported in Fig. 1b, were acquired to determine the effects of

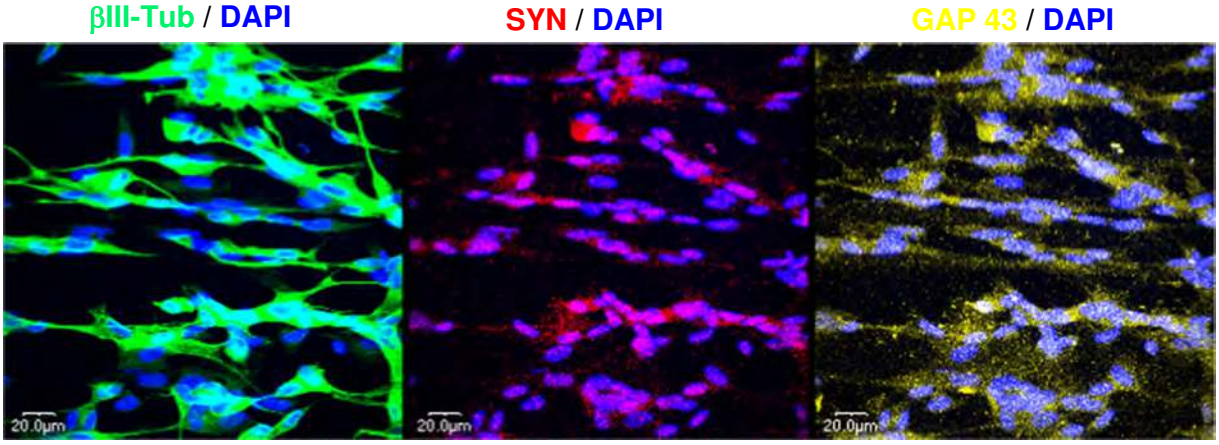

Fig. 3. PLLA-MTA membrane bioreactor supports neuronal growth and differentiation. Confocal laser micrographs of differentiated neuronal cells after 13 days of culture in PLLA-MTA membrane bioreactor. Cells were stained for neuronal markers βIII-tubulin (green), synaptophysin (red), and GAP-43 (yellow) and cell nuclei marker (DAPI, blue). (For interpretation of the references to colour in this figure legend, the reader is referred to the web version of this article.)

electrospun hollow fibers alignment on cell morphology under dynamic culture conditions. The cells in the bioreactor adhered onto the extra-fiber surface of PLLA-MTA membranes and displayed a neuronal-like morphology characterized by a spindle-like soma with considerable outgrowth of neurites able to sprout from the cell body along the membranes. The aligned PLLA-MTA membranes guided neurons into a defined aligned orientation according to the direction of the microtubes and allowed formation of neuronal network around the membranes, which are distinct features of developing neurons [30–32].

To confirm cell differentiation towards neuronal phenotype, the expression of several neuronal specific markers was assessed by confocal analysis. The significant expression of neuronal specific cytoskeletal proteins (βIII tubulin) joined to the high levels of growth-associated protein (GAP-43) expression, which is a marker of neuronal sprouting and axonal growth of mature neurons, in cells maintained for 2 weeks in bioreactor (Fig. 3), is indicative of activated signals essential for neuronal differentiation and maturation [33].

Synaptic formation is one of the hallmarks of mature neurons and can reflect the functional state of neuronal networks, thus, we have investigated the development of this structure to assess whether differentiated cells can actually behave as functional neurons. The punctate immunolocalization of synaptophysin along neuronal processes suggests the formation of active and functional synapses (Fig. 3). A complete neuronal maturation was further confirmed by the wide expression of markers associated to differentiated neurons as GAP43 and βIII Tub. PLLA-MTA bioreactor enabled the complex neuronal network, active synaptic formation, and recapitulation of neuronal maturation characteristics similar to those observed in vivo. Noteworthy, the neuronal phenotype was enhanced in bioreactor, both in terms of morphology and organization, and in terms of expression of neuronal markers.

In order to evaluate the capability of bioreactor to maintain specific neuronal functions, the metabolic activity of cells was investigated in terms of glucose consumption and BDNF secretion, and their concentration profiles were investigated by performing a modelling study. The experimental and modeled daily glucose concentration in the extraluminal compartment of the bioreactor, throughout the period of culturing neuronal cells under dynamic conditions, is reported in Fig. 4a. With an initial value of 1.3 mg/mL, the glucose concentration decreased in time almost linearly, reducing by ~ 25% after 7 days of culture. The simulated concentration profile of glucose within a cross-section PLLA-MTA membrane element of the bioreactor is shown in Fig. 4b. Due to its relatively low molecular weight (180 Da), glucose readily diffuses from microchannels to cellular compartment were consumption reaction takes place. The glucose consumption rate was almost constant at 4.5 ± 0.35 pg/cell·min for the duration of the culture period, suggesting that PLLA-MTA membrane bioreactor was able to sustain neuronal energy metabolism.

Additionally, we have also observed that the well-controlled microenvironment created by PLLA-MTA membrane bioreactor induced an increase of the concentration levels of well-known classical neurotrophic factors such as BDNF (Fig. 4c–d), an important mediator of neuronal survival and differentiation, both in vitro and in vivo.

According to Fig. 4c, the concentration of BDNF increases significantly in the first 6 days of secretion, and moderately in subsequent days; the behavior can be mathematically described by the following equation:

$$c_{BDNF} = \frac{A \bullet t}{B + t} \tag{2}$$

where c_{BDNF} is the concentration (pg/mL), A and B are fitting parameters (i.e. $3.15 \cdot 10^{-17}$ and 500, respectively), and t is the time (in minutes).

The simulated concentration profile of BDNF at day 8 is plotted in Fig. 4d. The diffusion coefficient of BDNF in aqueous medium, i.e. $3 \cdot 10^{-7}$ cm^2/s as calculated by the correlation proposed by Papadopoulos et al. [34] for a molecular weight of 27.8 kDa, is about 25 folds lower than glucose diffusivity. Effective BDNF diffusion coefficients is further reduced by the PLLA-MTA membrane porosity ($\varepsilon = 0.46$) [15]. As a consequence, mass transport is largely driven by convection, as confirmed by dimensionless Peclet number value $> 10^4$, and concentration difference between intraluminal and cellular layer is ~ 3.5%.

High values of the BDNF production rate were measured in neurons during the culture time within the bioreactor ($3.4 \cdot 10^{-5}$ pg/cell h).

These results are consistent with those found in literature. In the study of Pettingill et al. [35] on the survival-promoting effects of encapsulated BDNF over-expressing Schwann cells on auditory neurons in the deaf guinea pig control, enhanced green fluorescent protein (EGFP)-Schwann cells and post-transfected BDNF-Schwann cells had a BDNF production rate of 12.1 pg/day/10^6 cells (i.e.$5 \cdot 10^{-7}$ pg/cell h) and 568.1 pg/day/10^6 cells (i.e.$2.4 \cdot 10^{-5}$ pg/cell h). Investigation of Somoza et al. [36] on epigenetically generated BDNF-secreting hMSC revealed that exogenous addition of epidermal growth factor (EGF) and basic fibroblast growth factor (bFGF) induced BDNF release at rate of 125 pg/day/10^6 cells (i.e. $5.2 \cdot 10^{-6}$ pg/cell h).

It is interesting to note that cells inside the bioreactor maintained their functions up to 14 days of culture. This is due to the high membrane permeability properties and thin wall thickness that maximize the mass transfer exchange between cell and medium compartment thereby promoting cell viability and growth. Additionally, the

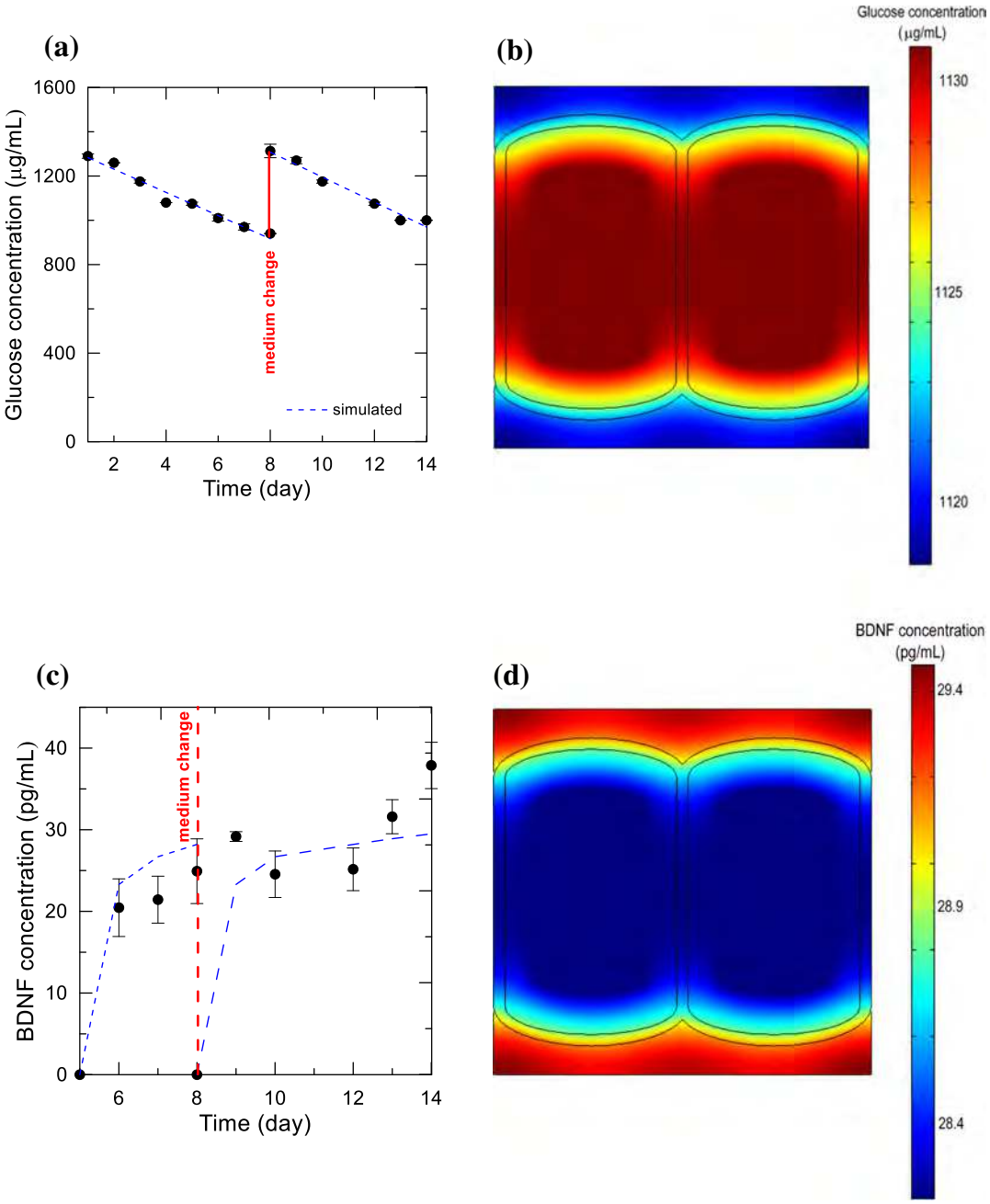

Fig. 4. Metabolic data of neurons evaluated as Glucose consumption (a–b) and BDNF secretion (c–d) up to 14 days. Time-dependent glucose concentration along 14 days of culture (a); simulated glucose concentration profile within MTA membrane element (b). Time variant BDNF concentration (dotted line: simulation results) (c); simulated BDNF concentration profile within MTA membrane element (d).

optimized fluid dynamic conditions ensure an adequate perfusion of nutrients and metabolites and the homogeneous distribution within the cell compartment avoiding shear stress phenomena. Furthermore, the distinct membrane array configuration characterized by highly aligned porous PLLA-MTA membranes, also provides guidance cues to direct cell orientation and enhance cell adhesion and differentiation.

As shown previously in the pioneering study [15], PLLA-MTA membrane bioreactor compartmentalized neuronal cells with directed neurite outgrowth and axonal processes within a three-dimensional (3-D) space that lead to control neuronal cell networking in vitro by promoting cellular response in terms of neuronal differentiation and neurite orientation.

Consistently with our previous work, herein, we demonstrated that PLLA-MTA membrane bioreactor provides a 3D low-shear stress environment for neuronal culture with enhanced diffusion of nutrients that successfully recapitulates developing neuronal-like tissue.

Thus, compared to other pioneering bioreactors, our device shows high reproducibility, which is critical to realize its promise as a standardized model for brain tissue. Therefore, this platform can be broadly used for drug testing, compound screening and disease modelling.

3.3. Neuronal PLLA-MTA membrane bioreactor as an in vitro model of Alzheimer's disease for testing Glycitein effects

The PLLA-MTA membrane bioreactor was employed to engineer functional neuronal tissue for disease modelling in order to provide effective experimental tool. In particular, in the present study, as an application of our membrane bioreactor-based platform for disease

modelling, we modeled the neurotoxicity associated to the most prevalent of neurodegenerative disorders, Alzheimer's disease, by reproducing in vitro the defining features of this neuropathology.

The aggregation of Amyloid-beta (Aβ) (1–42) is a key causative phenomenon closely related with the advent of Alzheimer's disease. Therefore, inhibition and/or prevention of Aβ-induced neurotoxicity is one of the most promising strategy for Alzheimer's disease treatment.

Several studies have shown that natural molecules with antioxidant and anti-amyloidogenic activity can play an important role in preventing the onset of the AD. Specifically, a soybean isoflavone with hormone-like properties (phytoestrogen), glycitein, has shown in in vivo and in vitro studies the ability to interact with β-amyloid peptides preventing the assembly of monomers and the formation of oligomers [37]. However, few information is available about its anti-amyloidogenic effects in neuronal cells.

Our approach was to use the neuronal PLLA-MTA membrane bioreactor as an in vitro model of Aβ -induced toxicity associated to Alzheimer's disease, to test the neuroprotective effect of the phytoestrogen glycitein. Particularly attention has been given to its potential effects against Aβ-induced neurotoxic events, such as cell death, ROS accumulation, and apoptosis, which result in neuronal dysfunction and death, and are characteristic features of Alzheimer's disease [38]. The results contribute to the better understanding of the neuroprotective effects of glycitein.

3.3.1. *Glycitein protects neurons against Aβ-induced toxicity in PLLA-MTA bioreactor*

Neuroprotection property of glycitein was assessed by co-treating differentiated neurons with 5 μM of Aβ (1–42) and different doses (25 μM, 50 μM and 100 μM) of Glycitein for 24 h, and then cell death was measured by MTT assay (Fig. 5a). Treatment of neurons with the toxic fragment of fibril Aβ (1–42) induced a significantly decrease ($p < 0.05$) of cell viability to 53 ± 0.9%, as compared to the control samples consisting of cells not treated with Aβ 1–42. By contrast, co-incubation with different concentrations of glycitein significantly increased cell viability which reached values similar to the control. The assay revealed that glycitein protected the viability of differentiated neurons by preventing cell death induced by Aβ (1–42) fragment.

To further investigate the neuroprotective action of glycitein, the effect on metabolic activity was also evaluated by measuring the glucose consumption in neurons after the different treatments (Fig. 5b). The administration of Aβ significantly reduced the consumption of glucose concentrations (31.87 ± 4.84 ng/cell) compared to the control (49.59 ± 6.5 ng/cell). On the contrary, glycitein treatment resulted in an increase of glucose consumed by neuronal cells, in the range of 51.84 ± 3.27 ng/cell and 55.25 ± 8.5 ng/cell, and restored the metabolic values of the control.

Therefore, the results show that glycitein inhibits cytotoxicity induced by β-amyloid both in terms of cell viability and metabolic functions.

3.3.2. *Glycitein scavenges Aβ-induced ROS production in neuronal cells in PLLA-MTA bioreactor*

Aβ-induced neurotoxicity also implicates oxidative stress that is associated with an increase of free radicals. In particular, several studies indicate the involvement and the damage caused by ROS in the pathogenesis of Alzheimer's, thus a correlation between the deposition of Aβ and the production of ROS has been observed.

The ability of glycitein to inhibit ROS production, induced by Aβ aggregation, has been investigated through the quantitative analysis of DCF in confocal microscopy, since the fluorescence emission of this molecule after oxidization following the acetylation is directly proportional to the amount of ROS produced by cells. The results reported in Fig. 6, show that the treatment of neuronal cells with Aβ significantly increased the DCF fluorescence intensity compared to the untreated cells. By contrast, glycitein administration at different concentrations

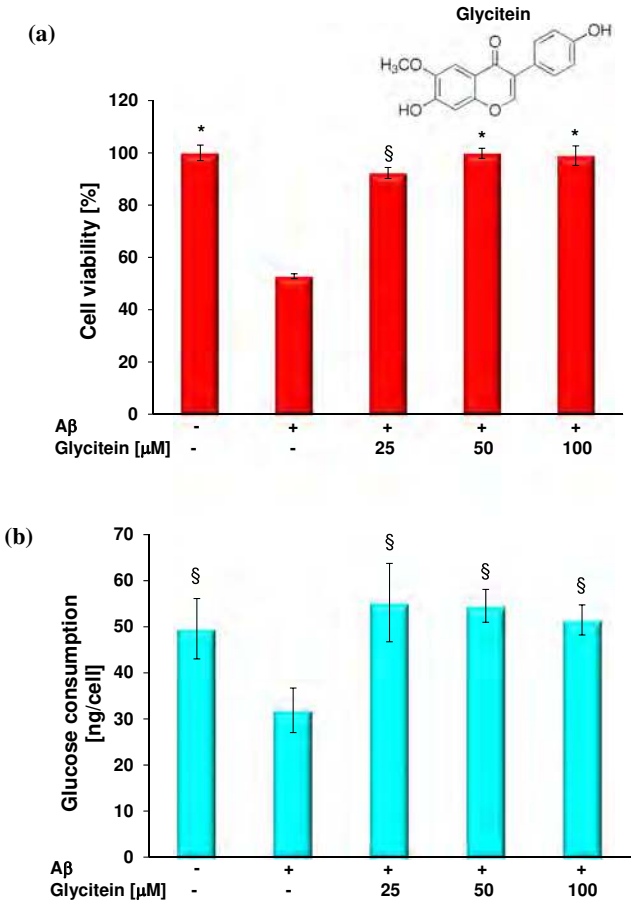

Fig. 5. Inhibitory effects of Glycitein on Aβ-induced cell damage in neuronal cells in PLLA-MTA membrane bioreactor. Glycitein protects neurons against Aβ-induced decrease of cell viability (a) and glucose consumption (b). The values expressed as average ± SD are the means of 3 experiments and data statistically significant were evaluated according to ANOVA followed by Bonferroni *t*-test ($p < 0.05$). * vs Aβ and Aβ + Glycitein 25 μM; $^{§}p < 0.05$ vs Aβ.

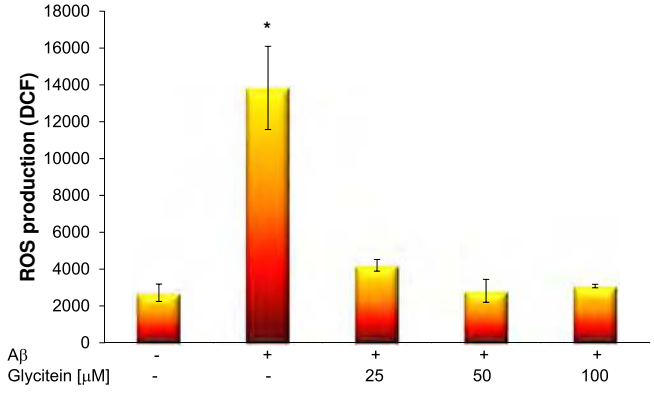

Fig. 6. Anti-oxidant effect of Glycitein. Quantitative analysis in confocal microscopy of ROS production expressed as fluorescence intensity of DCF produced at intracellular levels after 24 h of treatment with Aβ and glycitein at different concentrations. Data statistically significant according to ANOVA followed Bonferroni *t*-test. *$p < 0.05$ vs all treatments.

significantly reduced fluorescence intensity and, therefore, intracellular ROS production. Thus, this soy isoflavone glycitein protects neuronal cells by completely preventing Aβ-induced increase in intracellular ROS level, suggesting an antioxidant effect of the isoflavone. These findings are in agreement with an in vivo study in transgenic *Caenorhabditis*

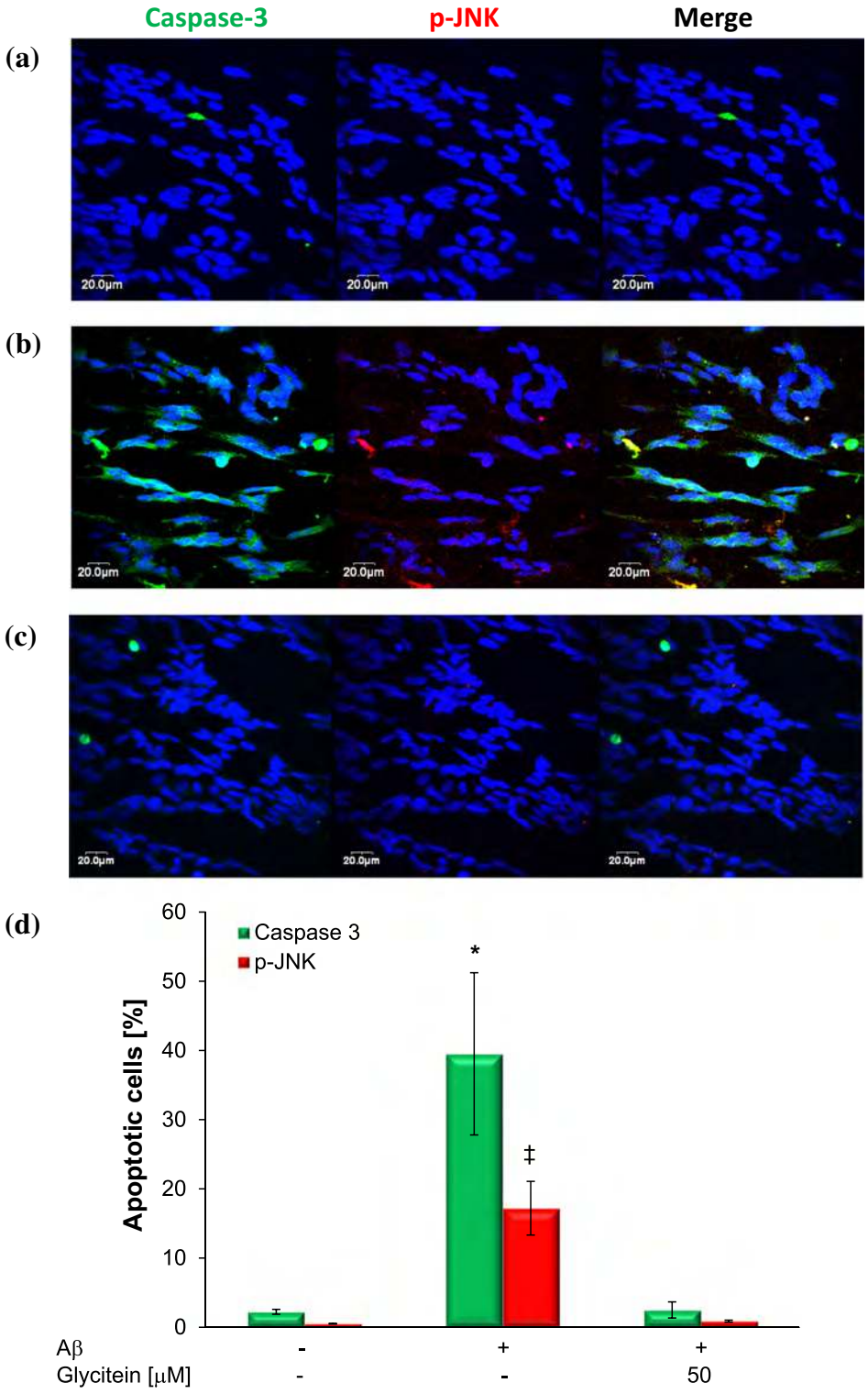

Fig. 7. Anti-apoptotic effect of Glycitein:
(a–c) Confocal Laser Scanning Microscopy (CLSM) representative images of neurons in PLLA-MTA membrane bioreactor in basal condition (no treatment) (a), after Aβ treatment (b) and after co-treatment with Aβ and Glycitein 50 µM (c). Cells were stained for apoptotic markers active caspase-3 (green), p-JNK (red) and nuclei (blue).
(d) Quantitative analysis of apoptotic markers Caspase-3 (green bar) and p-JNK (red bar). The values expressed as average ± SD are the means of 3 experiments and data statistically significant were evaluated according to ANOVA followed Bonferroni *t*-test ($p < 0.05$). For Caspase-3:* vs all treatments; for p-JNK: ‡ vs all treatments. (For interpretation of the references to colour in this figure legend, the reader is referred to the web version of this article.)

elegans by Zepeda et al. [39], that have demonstrated that glycitein suppressed Aβ toxicity through antioxidative activity by significantly attenuating ROS levels.

3.3.3. Glycitein inhibits Aβ-induced apoptosis in neuronal cells in PLLA-MTA bioreactor

Evidences support that Aβ-induced neurotoxicity is mediated by an apoptotic pathway which implicates the activation of specific signaling proteins. For example, the activation of JNK which is the sensor protein upstream of the apoptotic process due to ROS production, following the accumulation of amyloid in brain tissue, modulates the early signaling events involved in Aβ toxicity [40], and, caspase 3 is the major component mediating Aβ-induced apoptosis [41].

In the present work, in order to investigate the action of glycitein in protecting neuronal cells from the apoptotic pathway induced by Aβ aggregation, the expression of such critic apoptotic regulatory markers, caspase-3 and JNK, was evaluated. Fig. 7a–c report the confocal laser micrographs of the caspase-3 (in green) and p-JNK (in red) positive

neuronal cells, in PLLA-MTA membrane bioreactor-based tool, under different conditions. The toxicity of β-amyloid peptide induced the activation of both caspase-3 and phosphorylated JNK (Fig. 7b). On the contrary, these proteins were not expressed by neurons co-treated with Aβ and glycitein (50 μM) (Fig. 7c) in a similar fashion to neurons without treatment (control) (Fig. 7a).

A quantitative analysis of the number of positive cells at caspase-3 and p-JNK compared to the total number of cells confirmed these results. The Aβ treatment produced a significant increase in apoptotic cells expressing both caspase-3 and p-JNK with values of 39.5 ± 11.7% and 17.20 ± 3.87%, respectively (Fig. 7d). On the other hand, the administration of glycitein at a concentration of 50 μM significantly reduced the percentages of apoptotic cells for caspase-3 and p-JNK to values of 2.5 ± 1.16% and 0.88 ± 0.14%, respectively, which are comparable to those detected in neurons not exposed to any insult.

As already demonstrated for other phytoestrogens in cortical neurons [41], also glycitein neuroprotective effect against Aβ toxicity is mediated by the inhibition of caspase cascade. In addition, for the first time, our data provide also evidence about the inhibitory effect of glycitein against Aβ-induced apoptosis by abrogating JNK activation. In our PLLA-MTA bioreactor-based tool, the increased levels of cleaved caspase 3 and phosphorylated JNK were completely suppressed by glycitein suggesting that isoflavone inhibits the activation of both apoptotic markers.

In summary, our findings provide several lines of evidence that glycitein protects neuronal cells by inhibiting Aβ-induced neurotoxicity.

Previous works have demonstrated the anti-aggregating capacity of glycitein in vivo [39] and in vitro in solutions containing the isoflavone and Aβ without any cell system [37]. Therefore, in the literature, there are no other studies investigating the protective effect against Aβ-induced toxic events in neuronal cells. In the present work, thanks to the use of PLLA-MTA bioreactor-based tool, the ability of glycitein of inhibiting the toxicity induced by Aβ aggregation was tested for the first time in neuronal cells in vitro.

Some reports have demonstrated that polyphenol compounds exhibit inhibitory effects on Aβ aggregation by binding hydrophobic β-sheet channels with their aromatic structure and simultaneously disturb Aβ hydrogen bond formation through the action of hydroxyls as electron donors [42]. Glycitein is chemically composed of a diphenolic structure with polyhydroxyl groups (Fig. 5a) and may function through the above mechanisms. Therefore, according to the study conducted by Hirohata et.al [37], the neuroprotective activity of glycitein could be related to its chemical structure by the interaction with the $A\beta_{1-42}$ peptide which prevents the addition of monomers, the assembly of amyloid and, therefore, the formation of amyloidogenic plaques. The anti-fibrillation and anti-oligomerization effects of glycitein could be due to its directly interaction with monomers, oligomers and fibrils of $A\beta_{1-42}$. Glycitein initially binds with the sites present in monomeric Aβ peptide, thereby preventing fibrillation and oligomerization. Alternatively, glycitein binds to Aβ fibrils or oligomers, thus inhibiting the addition of Aβ monomers onto the growing ends of Aβ assembly.

Our findings validate neuronal PLLA-MTA membrane bioreactor as in vitro investigational tool for testing the neuroprotective effect of new therapeutic compounds. Indeed although most hollow fiber bioreactor-based models have been developed for various organs and disease states, such as liver, blood brain barrier and kidney [43], their use as in vitro investigational platform for neurodegenerative disease is still to an unsatisfactory state.

To our knowledge, the PLLA-MTA bioreactor realized in the present study together with the previous one, PAN-HF membrane bioreactor [14], so far are the first examples of advanced bioreactor-based tools successfully employed as in vitro model of Alzheimer's disease and designed for therapeutic use. Furthermore, PLLA-MTA bioreactor compared to PAN-HF bioreactor has also the advantage to support and guide neurite orientation, which is crucial for neuronal regeneration.

4. Conclusions

This work showed how the high mass transfer, the low shear stress and 3-D homogeneous and stable in vitro microenvironment within the PLLA-MTA membrane bioreactor provide optimal conditions for the growth and differentiation of neural cells, as well as for the long-term maintenance of their metabolic functions. Several findings have been achieved in the present study. The creation of a 3D neuronal in vitro model, allows using the PLLA-MTA membrane bioreactor as reliable investigational platform for the study of neurodegeneration mechanisms for the preclinical evaluation of new therapeutics. Overall, our findings provide important and further insights underlying the neuroprotective effects of the isoflavone glycitein. Treatment with glycitein inhibits the cytotoxic event triggered by β-amyloid while maintaining high cell viability, reduces the number of cells in apoptosis by inactivating specific protein markers and protects against ROS production by highlighting an antioxidant action. Our results support the hypothesis that soybean isoflavone glycitein could have potential effect in preventing one of the critical events in the physiopathology of Alzheimer's disease, since accumulation of Aß aggregates is the primary cause of neuronal dysfunction.

The present study contributed also to confirm that the development of neuroprotective agents such as a compound that combines potent antioxidant and apoptotic inhibitory properties might prevent the incidence or retard the progression of Alzheimer's disease.

In conclusion, models based on the implementation of advanced engineered systems, such as membrane bioreactors, in which neurons are cultured within a dynamic device designed to recapitulate specific microenvironment of living neuronal tissue, have great potential as complementary tools in preclinical research, contributing to expand the available in vitro devices for drug screening.

References

[1] F.G. Teixeira, N.L. Vasconcelos, E.D. Gomes, F. Marques, J.C. Sousa, N. Sousa, N.A. Silva, R. Assuncao-Silva, R. Lima, A.J. Salgado, Bioengineered cell culture systems of central nervous system injury and disease, Drug Discov. Today 21 (2016) 1456–1463.
[2] P. Zhuang, A.X. Sun, J. An, C.K. Chua, S.Y. Chew, 3D neural tissue models: from spheroids to bioprinting, Biomaterials 154 (2018) 113–133.
[3] H. Moradian, H. Keshvari, H. Fasehee, R. Dinarvand, S. Faghihi, Combining NT3-overexpressing MSCs and PLGA microcarriers for brain tissue engineering: a potential tool for treatment of Parkinson's disease, Mater. Sci. Eng. C Mater. Biol. Appl. 76 (2017) 934–943.
[4] A.R. Murphy, A. Laslett, C.M. O'Brien, N.R. Cameron, Scaffolds for 3D in vitro culture of neural lineage cells, Acta Biomater. 54 (2017) 1–20.
[5] P. Sensharma, G. Madhumathi, R.D. Jayant, A.K. Jaiswal, Iomaterials and cells for neural tissue engineering: current choices, Mater. Sci. Eng. C Mater. Biol. Appl. 77 (2017) 1302–1315.
[6] S. Morelli, A. Piscioneri, S. Salerno, E. Drioli, L. De Bartolo, Biohybrid membrane systems for testing molecules and stem cell therapy in neuronal tissue engineering, Curr. Pharm. Des. 23 (2017) 3858–3870.
[7] M. Mele, S. Morelli, G. Fazzari, E. Avolio, R. Alò, A. Piscioneri, L. De Bartolo, R.M. Facciolo, M. Canonaco, Application of the co-culture membrane system pointed to a protective role of catestatin on hippocampal plus hypothalamic neurons exposed to oxygen and glucose deprivation, Mol. Neurobiol. 54 (2017) 7369–7381.
[8] A. Piscioneri, S. Morelli, M. Mele, M. Canonaco, E. Bilotta, P. Pantano, E. Drioli, L. De Bartolo, Neuroprotective effect of human mesenchymal stem cells in a compartmentalized neuronal membrane system, Acta Biomater. 24 (2015) 297–308.
[9] S. Morelli, A. Piscioneri, S. Salerno, M. Al-Fageeh, E. Drioli, L. De Bartolo, Neuroprotective effect of didymin on H_2O_2-induced injury in neuronal membrane system, Cells Tissues Organs 199 (2014) 184–200.
[10] G. Giusi, R.M. Facciolo, M. Rende, R. Alo, A. Di Vito, S. Salerno, S. Morelli, L. De Bartolo, E. Drioli, M. Canonaco, Distinct α subunits of the GABAA receptor are responsible for early hippocampal silent neuron-related activities, Hippocampus 19 (2009) 1103–1114.
[11] J. Teng, M. Zhang, K.T. Leung, J. Chen, H. Hong, H. Lin, B.Q. Liao, A unified thermodynamic mechanism underlying fouling behaviors of soluble microbial products (SMPs) in a membrane bioreactor, Water Res. 149 (2019) 477–487.
[12] J. Teng, L. Shen, Y. He, B.Q. Liao, G. Wu, H. Lin, Novel insights into membrane fouling in a membrane bioreactor: elucidating interfacial interactions with real membrane surface, Chemosphere 210 (2018) 769–778.

[13] J. Chen, M. Zhang, F. Li, L. Qian, H. Lin, L. Yang, X. Wu, X. Zhou, Y. He, B.Q. Liao, Membrane fouling in membrane bioreactor: high filtration resistance of gel layer and its underlying mechanism, Water Res. 102 (2016) 82–89.
[14] S. Morelli, Simona Salerno, Antonella Piscioneri, Franco Tasselli, E. Drioli, L. De Bartolo, Neuronal membrane bioreactor as a tool for testing crocin neuroprotective effect in Alzheimer's disease, Chem. Eng. J. 305 (2016) 69–78.
[15] S. Morelli, A. Piscioneri, S. Salerno, C.C. Chen, C.H. Chew, L. Giorno, E. Drioli, L. De Bartolo, Microtube array membrane bioreactor promotes neuronal differentiation and orientation, Biofabrication 9 (2017) 025018, , https://doi.org/10.1088/1758-5090/aa6f6f.
[16] E. Curcio, A. Piscioneri, S. Salerno, F. Tasselli, S. Morelli, E. Drioli, L. De Bartolo, Human lymphocytes cultured in 3-D bioreactors: influence of configuration on metabolite transport and reactions, Biomaterials 33 (2012) 8296–8303.
[17] C.A. Brayfield, K.G. Marra, J.P. Leonard, X.T. Cui, J.C. Gerlach, Excimer laser channel creation in polyethersulfone hollow fibers for compartmentalized in vitro neuronal cell culture scaffolds, Acta Biomater. 4 (2008) 244–255.
[18] C.A. Rodrigues, M.M. Diogo, C.L. da Silva, J.M. Cabral, Microcarrier expansion of mouse embryonic stem cell-derived neural stem cells in stirred bioreactors, Cabral Biotechnol. Appl. Biochem. 58 (2011) 231–242.
[19] J. Vukasinovic, D.K. Cullen, M.C. LaPlaca, A. Glezer, A microperfused incubator for tissue mimetic 3D cultures, Biomed. Microdevices 11 (2009) 1155–1165.
[20] G. Jin, R. He, B. Sha, W. Li, H. Qing, R. Teng, F. Xu, Electrospun three-dimensional aligned nanofibrous scaffolds for tissue engineering, Mater. Sci. Eng. C Mater. Biol. Appl. 92 (2018) 995–1005.
[21] W.C. Hung, L.H. Lin, W.C. Tsen, H.S. Shie, H.L. Chiu, T.C.K. Yang, C.C. Chen, Permeation of biological compounds through porous poly(L-lactic acid) (PLLA) microtube array membranes (MTAMs), Eur. Polym. J. 67 (2015) 166–173.
[22] S. Morelli, S. Salerno, J. Holopainen, M. Ritala, L. De Bartolo, Osteogenic and osteoclastogenic differentiation of cocultured cells in polylactic acid-nanohydroxyapatite fiber scaffolds, J. Biotechnol. 204 (2015) 53–62.
[23] S. Morelli, A. Piscioneri, A. Messina, S. Salerno, M.B. Al-Fageeh, E. Drioli, L. De Bartolo, Neuronal growth and differentiation on biodegradable membranes, J. Tissue Eng. Regen. Med. 1 (2015) 106–117.
[24] J.Y. Park, S.K. Kim, D.H. Woo, E.J. Lee, J.H. Kim, S.H. Lee, Differentiation of neural progenitor cells in a microfluidic chip- generated cytokine gradient, Stem Cells 27 (2009) 2646e54.
[25] T. DiStefano, H.Y. Chen, C. Panebianco, K.D. Kaya, M.J. Brooks, L. Gieser, N.Y. Morgan, T. Pohida, A. Swaroop, Accelerated and improved differentiation of retinal organoids from pluripotent stem cells in rotating-wall vessel bioreactors, Stem Cell Rep. 10 (2018) 300–313.
[26] C.M. Valmikinathan, J. Hoffman, X. Yu, Impact of scaffold micro and macro architecture on schwann cell proliferation under dynamic conditions in a rotating wall vessel bioreactor, Mater. Sci. Eng. C Mater. Biol. Appl. 31 (2011) 22–29.
[27] S. Morelli, A. Piscioneri, E. Drioli, L. De Bartolo, Neuronal differentiation modulated by polymeric membrane properties, Cells Tissues Organs 204 (2017) 164–178.
[28] L. De Bartolo, S. Morelli, A. Bader, E. Drioli, Evaluation of cell behaviour related to physico-chemical properties of polymeric membranes to be used in bioartificial organs, Biomaterials 23 (2002) 2485–2497.
[29] L. De Bartolo, A. Piscioneri, G. Cotroneo, S. Salerno, F. Tasselli, C. Campana, S. Morelli, M. Rende, M.C. Caroleo, M. Bossio, E. Drioli, Human lymphocyte PEEK-WC hollow fiber membrane bioreactor, J. Biotechnol. 132 (2007) 65–74.
[30] S. Morelli, A. Piscioneri, S. Salerno, F. Tasselli, A. Di Vito, G. Giusi, M. Canonaco, E. Drioli, L. De Bartolo, PAN hollow fiber membranes elicit functional hippocampal neuronal network, J. Mater. Sci. Mater. Med. 23 (2012) 149–156.
[31] S. Morelli, A. Piscioneri, S. Salerno, M. Rende, C. Campana, F. Tasselli, A. di Vito, G. Giusi, M. Canonaco, E. Drioli, L. De Bartolo, Flat and tubular membrane systems for the reconstruction of hippocampal neuronal network, J. Tissue Eng. Regen. Med. 6 (2012) 299–313.
[32] S. Morelli, S. Salerno, A. Piscioneri, B.J. Papenburg, A. Di Vito, G. Giusi, M. Canonaco, D. Stamatialis, E. Drioli, L. De Bartolo, Influence of micro-patterned PLLA membranes on outgrowth and orientation of hippocampal neurites, Biomaterials 31 (2010) 7000–7011.
[33] O. Avwenagha, G. Campbell, M.M. Bird, Distribution of GAP-43, beta-III tubulin and F-actin in developing and regenerating axons and their growth cones in vitro, following neurotrophin treatment, J. Neurocytol. 32 (2003) 1077–1089.
[34] S. Papadopoulos, K.D. Jürgens, G. ,ros G. Protein diffusion in living skeletal muscle fibers: dependence on protein size, fiber type, and contraction, Biophys. J. 79 (2000) 2084–2094.
[35] L.N. Pettingill, A.K. Wise, M.S. Geaney, R.K. Shepherd, Enhanced auditory neuron survival following cell-based BDNF treatment in the deaf Guinea pig, PLoS One 6 (2011) e18733.
[36] R. Somoza, C. Juri, M. Baes, U. Wyneken, F.J. Rubio, Intranigral transplantation of epigenetically induced BDNF-secreting human mesenchymal stem cells: implications for cell-based therapies in Parkinson's disease, Biol. Blood. Marrow Transplant. 16 (2010) 1530–1540.
[37] M. Hirohata, K. Ono, J. Takasaki, R. Takahashi, T. Ikeda, A. Morinaga, M. Yamada, Anti-amyloidogenic effects of soybean isoflavones in vitro: fluorescence spectroscopy demonstrating direct binding to Aβ monomers, oligomers and fibrils, Biochim. Biophys. Acta 1822 (2012) 1316–1324.
[38] J. Hardy, D.J. Selkoe, The amyloid hypothesis of Alzheimer's disease: progress and problems on the road to therapeutics, Science 297 (2002) 353–356.
[39] A. Gutierrez-Zepeda, R. Santell, Z. Wu, M. Brown, Y.J. Wu, I. Khan, C.D. Link, B. Zhao, Y. Luo, Soy isoflavone glycitein protects against beta amyloid-induced toxicity and oxidative stress in transgenic Caenorhabditis elegans, BMC Neurosci. 6 (2005) 54, https://doi.org/10.1186/1471-2202-6-54.
[40] M. Yao, T.V. Nguyen, C.J. Pike, Beta-amyloid-induced neuronal apoptosis involves c-Jun N-terminal kinase-dependent downregulation of Bcl-w, J. Neurosci. 25 (2005) 1149–1158.
[41] C.N. Wang, C.W. Chi, Y.L. Lin, C.F. Chen, Y.J. Shiao, The neuroprotective effects of phytoestrogens on amyloid β protein-induced toxicity are mediated by abrogating the activation of caspase cascade in rat cortical neurons, J. Biol. Chem. 276 (2001) 5287–5295.
[42] S.G. Yang, X. Zhang, X.S. Sun, T.J. Ling, Y. Feng, X.Y. Du, M. Zhao, Y. Yang, D. Xue, L. Wang, R.T. Liu, Diverse ecdysterones show different effects on amyloid-β42 aggregation but all uniformly inhibit amyloid-β42-induced cytotoxicity, J. Alzheimers Dis. 22 (2010) 107–117.
[43] M. Ginai, R. Elsby, C.J. Hewitt, D. Surry, K. Fenner, K. Coopman, The use of bioreactors as in vitro models in pharmaceutical research, Drug Discov. Today 18 (2013) 922–935.